Thermochimica Acta 494 (2009) 30–34

Contents lists available at ScienceDirect

Thermochimica Acta

journal homepage: www.elsevier.com/locate/tca

The influence of reductant on the crystallization of CaO–MgO–SiO_2 glass

Peijing Tian*, Jinshu Cheng, Weihong Zheng, Hong Li

Key Laboratory for Silicate Materials Science and Engineering of Ministry of Education, Wuhan University of Technology, Wuhan 430070, China

ARTICLE INFO

Article history:
Received 22 January 2009
Received in revised form 14 April 2009
Accepted 16 April 2009
Available online 24 April 2009

Keywords:
Reductant
Glass ceramics
Diopside
Crystallization

ABSTRACT

The effect of reductant on the crystallization of CaO–MgO–SiO_2 glass was investigated by XRD, SEM, EDS and DTA. The $CaMgSi_2O_6$ phase was identified by heat treatment of the investigated glasses, and the restrained crystallization was observed in the investigated glass with additional $C_{12}H_{22}O_{11}$. It is indicated that the glasses were prone to surface crystallization, and the inhibited crystallization was caused by the lack of oxygen in the core of the glass added reductant. The kinetic analysis showed that $C_{12}H_{22}O_{11}$ restrained the crystallization of CaO–MgO–SiO_2 glass with increasing the crystallization peak temperature (T_p) and activation energy (E).

1. Introduction

In recent years, glass and glass ceramics of the CaO–MgO–SiO_2 system have attracted great interest due to their durability, mechanical and biomedical properties arising from the precipitation of diopside, wollastonite and melilite phase [1–3]. And the diopside or melilite glass ceramics has potential application on the optical devices [4–6], due to the luminescence properties and long afterglow phenomenon of $Ca_2MgSi_2O_7$:Eu^{2+},Dy^{3+} [7], $CaMgSi_2O_6$:Eu^{2+},Dy^{3+} [8]. According to the previous report [9–13], glass of this system are always prone to surface crystallization, but the mechanisms and kinetics of surface nucleation are not well understood so far [12,13].

In order to obtain special performance, sometimes the raw materials of glass need to be melted under reducing atmosphere, such as producing glass ceramics doped with low valence ions. But the crystallization of glass may be affected by the atmosphere [12], especially for the glass whose devitrification starts from surface. For example, Partridge and McMillan [14] reported that the surface crystallization of ZnO–Al_2O_3–SiO_2 glass was inhibited if the ambient did not include O_2 or H_2O vapor.

There is another way to melt glass under reduction atmosphere — just by adding reducing agents, we can avoid using inert gases in special furnaces when we melt the glasses. But the role of reducing agents on the crystallization of silicate glasses has not been studied. Therefore, study about reductant influence on crystallization behavior becomes necessary for this kind of glass.

The influence of the reductant on the crystallization of CaO–MgO–SiO_2 glass is not completely clear to our knowledge. In this paper, glass ceramics based on the CaO–MgO–SiO_2 system were prepared, $C_{12}H_{22}O_{11}$ was chosen to be the reductant, which will not introduce any additional impurity. The results indicate that something interesting is going on after adding reductant. And the influences of $C_{12}H_{22}O_{11}$ on the structure and crystallization kinetic characteristics were also investigated.

2. Experimental procedure

The glass composition comprised 17.5CaO–14.5MgO–58.5SiO_2–4.0Al_2O_3–1.0B_2O_3 –3.0ZnO–1.0Na_2O–0.5ZrO_2 (in mol%), the reduction atmosphere was produced by the addition of $C_{12}H_{22}O_{11}$. Reagent-grade $CaCO_3$, MgO, SiO_2, Al_2O_3, H_3BO_3, ZnO, Na_2CO_3, ZrO_2, $C_{12}H_{22}O_{11}$ were used as raw materials. Batch of 100 g were weighed and mixed in a ball mill for 3 h, and the milling was carried out in an agate mortar with agate balls, then the raw materials were placed into Pt crucible. In order to avoid the reductant loss, the batches were put into the electric furnace at 1500 °C and melted at this temperature for 2 h. Blocks of bulk transparent glasses were produced by easy casting of melts on preheated steel moulds and then immediate annealing at 550 °C for 1 h. After furnace-cooling, the glass was cut into rectangular pieces of 25 mm × 20 mm × 10 mm and their surfaces were polished with 3 to 4 μm diameter diamond paste. The obtained glass was re-heated at 854–1100 °C for 180 min and cooled down to room temperature. Compared with the colorless transparent samples without heat treatment, the samples after heat treatment were all transparent glass with white opaque on the surface, and the crystalline layer thickness increased with the increasing heat treatment temperature. The content of sucrose,

* Corresponding author. Tel.: +86 027 87860801; fax: +86 027 87860801.
E-mail address: peijingtian@yahoo.com.cn (P. Tian).

0040-6031/$ – see front matter © 2009 Elsevier B.V. All rights reserved.
doi:10.1016/j.tca.2009.04.013

Table 1
Composition and heat treatment temperature of samples.

No.	Added content of $C_{12}H_{22}O_{11}$ (g)	Heat treatment temperatures (°C)	Crystalline layer thickness (mm)
A0	0	Not be heat-treated	0
A1	0	854	0.68
A2	0	964	1.96
A3	0	1100	4.44
R0	10	Not be heat-treated	0
R1	10	854	0
R2	10	875	0.52
R3	10	1013	1.27
R4	10	1100	2.60

the crystalline layer thickness and heat treatment temperature are listed in Table 1.

The samples were ground to powder and subjected to pass 200 meshes sieve in order to identify the crystalline phases by X-ray diffraction method. The experiments were conducted on a Rigaku D/Max-IIIA X-ray diffractometer, which produced at 35 kV and 30 mA, scanned the range of diffraction angles (2θ) between 10° and 60° with a 2θ-step of 0.02° per second, copper Kα radiation. Scanning electron microscopy (SEM, JEOL JSM-5610LV, Japan) equipped with energy disperse spectrometry (EDS) was employed for microstructure observations and elemental analysis at etched section (by immersion in 3 vol.% HF solution for 5 min). Differential thermal analysis (DTA, Netzsch STA 449C, Germany) of annealed glass samples was carried out in a nitrogen atmosphere using an Al_2O_3 powder reference standard and heating rates of 5, 10, 15 and 20 °C min^{-1} from room temperature to 1100 °C.

3. Results and discussion

3.1. Influence on crystallization

Fig. 1 shows the DTA curves with exothermic crystallization peaks for samples A0 and R0 at heating rate of 10 °C min^{-1}. The DTA curve of sample A0 shows a small endothermic peak valley at 742 °C, a major peak at 854 °C and a shoulder peak at 964 °C. And the DTA trace of the R0 specimen exhibits an endothermic peak valley at 747 °C, two major peaks at 875 °C and 1013 °C. The first peak implies the glass transition temperature (T_g), and the second and third peaks are attributed to the crystallization (T_p) or transformation of crystal structure. The T_g and T_p of the glasses shift to higher temperature after adding $C_{12}H_{22}O_{11}$. The crystallization peaks on

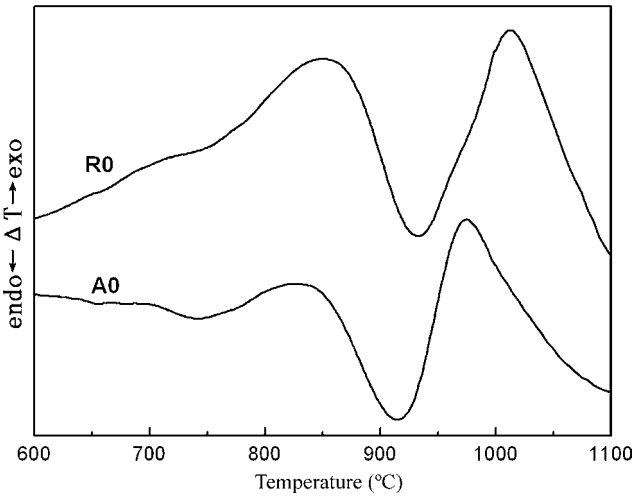

Fig. 1. DTA curves of sample A0 and R0 at heating rate of 10 °C min^{-1}.

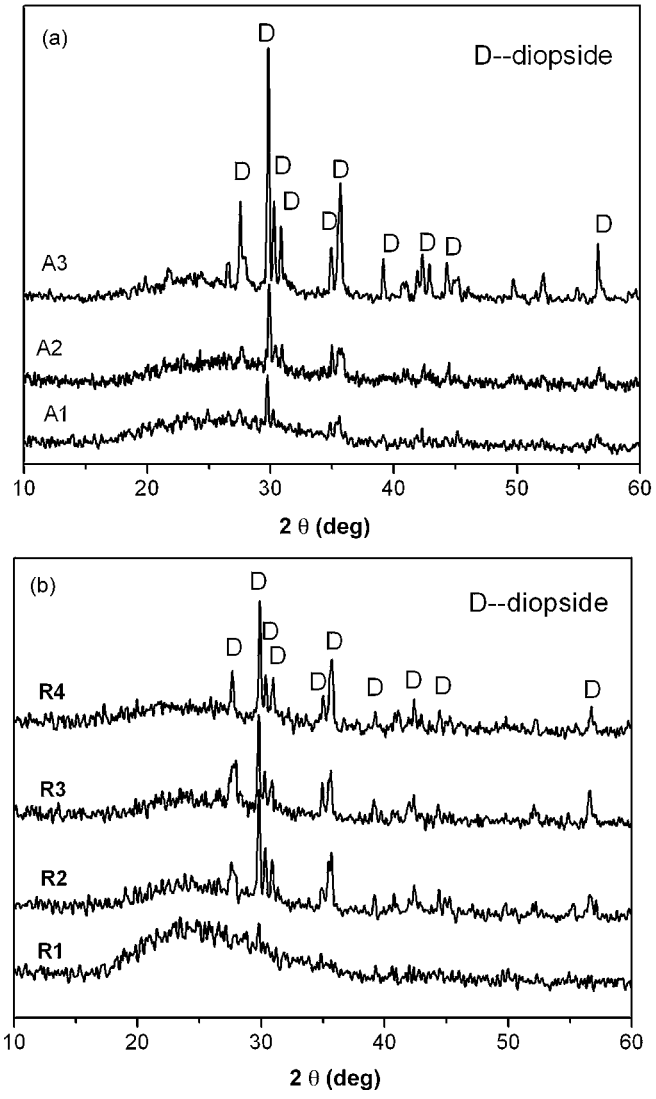

Fig. 2. XRD pattern for samples. D, diopside($CaMgSi_2O_6$,72-1497).

the DTA curves imply that crystalline phase forms during the heat treatment.

Fig. 2 shows the diffraction patterns of samples treated at different temperatures for 3 h according to their DTA curves. After heat treated at 854 °C, diopside crystals were precipitated in glass. So the first crystallization peak in DTA can be recognized as the crystallization peak temperature of diopside. As the temperature increases from 854 to 1100 °C, the content of diopside in $C_{12}H_{22}O_{11}$-free samples increases gradually. XRD patterns of R1 after treated at 854 °C show a broad scattering spectrum and the main phase is still amorphous glass. After heated at higher temperatures (R2-R3), the broad scattering spectrum disappears and diopside precipitates. As the heated temperature increases to 1100 °C, diopside is still the main phase. The crystal phase had no change after the addition of $C_{12}H_{22}O_{11}$, which means the main crystal phase is not influenced by the reductant in CaO–MgO–SiO_2 glass ceramics. Nevertheless, when we compared sample A1 with R1 heat treated at the same temperature, there was a remarkable distinction in their XRD pattern, diopside was recognized in A1 but was not found in R1. For A3 and R4, higher XRD peaks intensity was observed in A3. The data in Table 1 also showed that the crystalline layer thickness decreased after adding $C_{12}H_{22}O_{11}$ to glass even though they experienced the same heat treatment process. These results

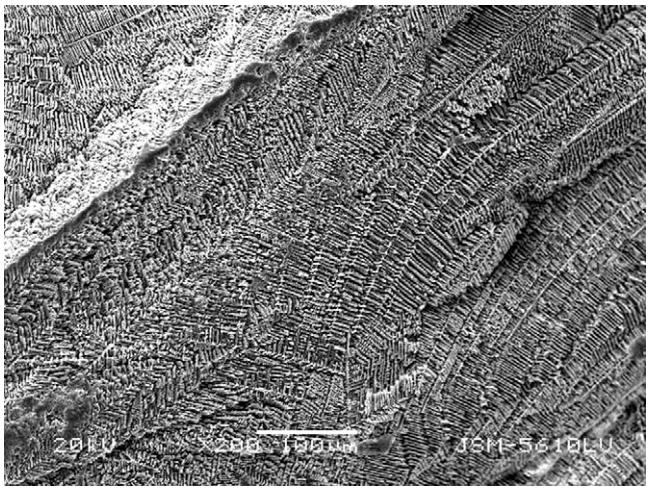

Fig. 3. SEM micrograph of the glass ceramics no. A3.

indicate that crystallization is more difficult in glass introducing $C_{12}H_{22}O_{11}$.

3.2. Microstructure

The microstructure of the glass ceramics (sample A3) before the addition of $C_{12}H_{22}O_{11}$ is shown in Fig. 3. Fibrous crystals arranged regularly were observed, which showed the characteristic of directional crystallization of the glass. And the interface between two crystalline layers was also observed significantly. The micrograph at higher magnification is shown in Fig. 4. The integrity of these crystals was obviously noticed, and the EDS analysis (Fig. 5) reveals that the main crystalline phase appeared as fine crystals is diopside in sample A3.

The SEM micrograph of the glass ceramics (sample R4) introduced by the $C_{12}H_{22}O_{11}$ are shown in Figs. 6 and 7. Fig. 6 shows the morphology at the interface between glass and crystal phase in sample R4, the crystal phase advanced slowly towards the core of the bulk glass, confirming that the glass are prone to surface crystallization. And the bulk of the glass at higher magnification is shown in Fig. 7. Two-dimensional dendritic growth of crystallization on the surface was observed. Compared with the fibrous crystals arranged regularly in sample A3, crystals in sample R4 formed a fractal pattern, which developed with a typical multi-branching tree-like form. But part of the crystals which arranged

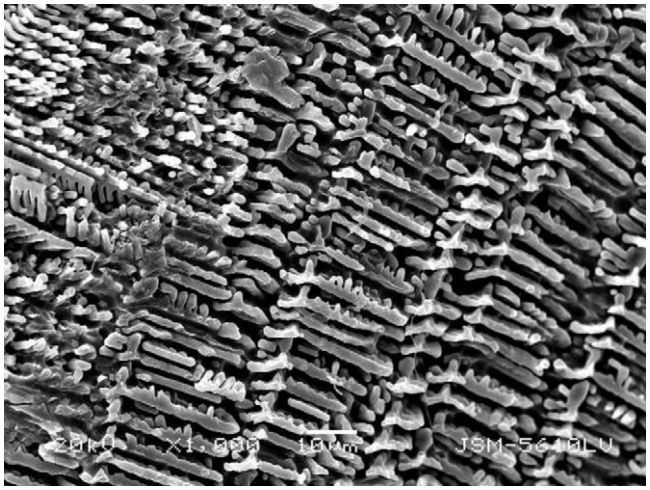

Fig. 4. SEM micrograph of the glass ceramics no. A3 at higher magnification.

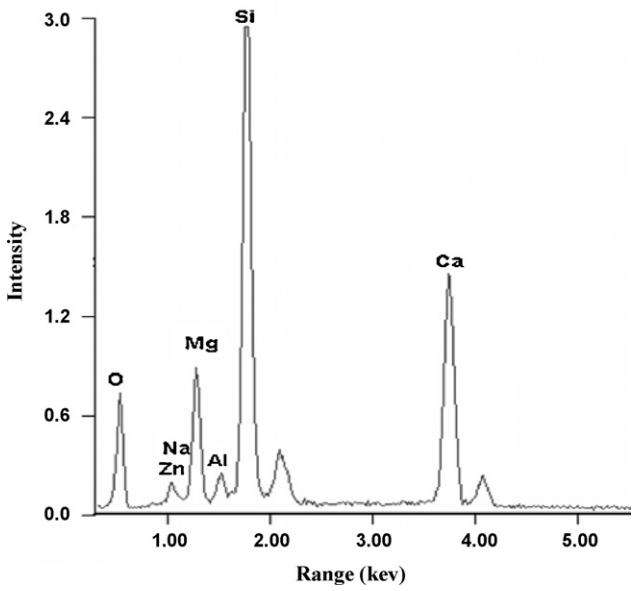

Fig. 5. The EDS analysis of the diopside in glass ceramics no. A3.

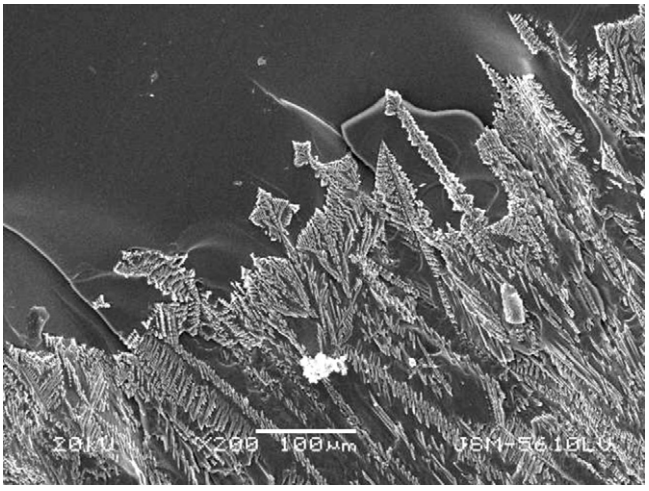

Fig. 6. SEM micrograph of the glass ceramics no. R4. The outer surface of the sample is at the bottom of the image.

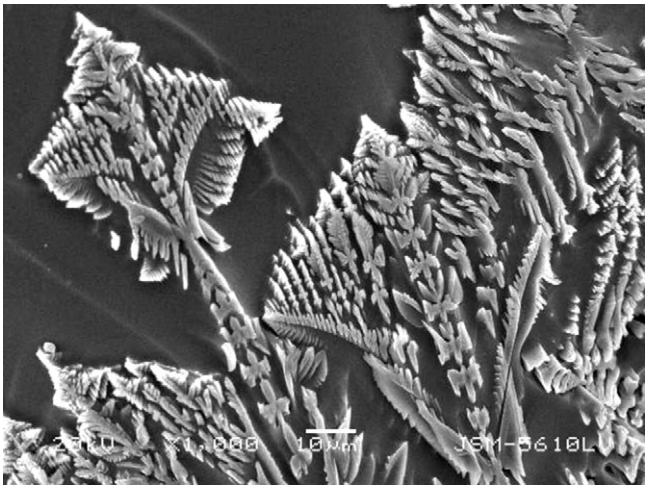

Fig. 7. SEM micrograph of the glass ceramics no. R4 at higher magnification.

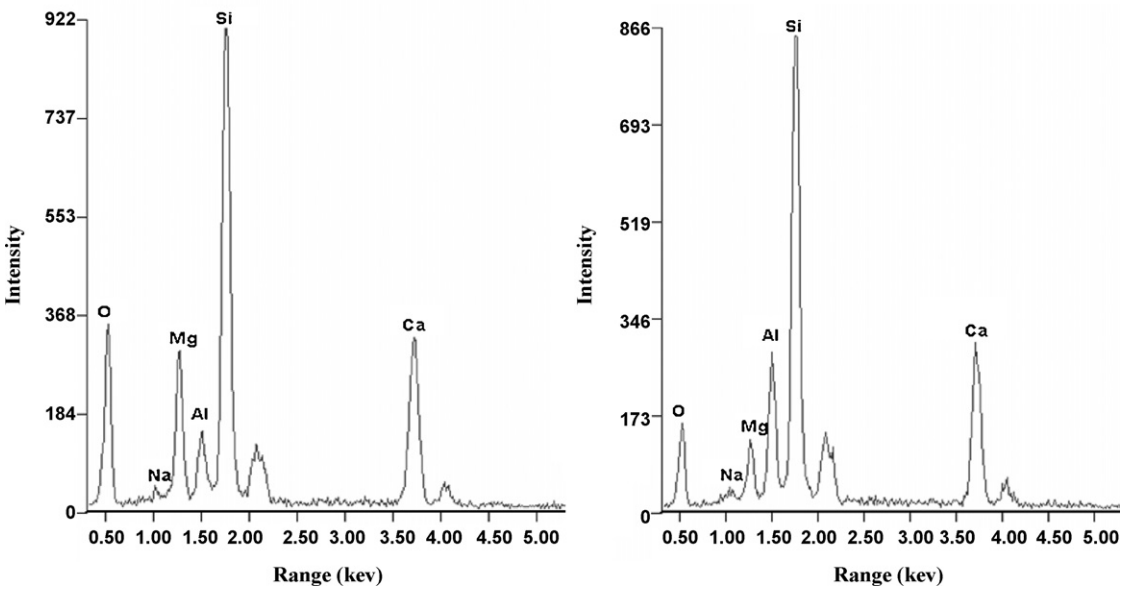

Fig. 8. The EDS analysis of glass ceramics no. R4: (a) diopside; (b) glass phase.

regularly and directionally were observed, which means the crystals are not fully developed in sample R4. So the crystal growth is obviously restrained in the glass ceramics added $C_{12}H_{22}O_{11}$.

EDS analysis of the crystal and glass phase in sample R4 is shown in Fig. 8a and b. As shown in Fig. 8a, diopside was identified as the white opaque in the surface of sample R4. Fig. 8b shows the presence of the elements O, Mg, Al, Si and Ca in the glass phase, and the glass phase had lower oxygen content and higher aluminum content than those in the crystal phase. $CaMgSi_2O_6$ phase contains less Al, which is comprehensible, consequently the change of oxygen content is responsible for the inhibited crystallization. This observation indicates that the inhibited crystallization is affected by the lack of oxygen in the core of the glass added $C_{12}H_{22}O_{11}$. A possible explanation is that nearly all of the aluminum ions are present in the form of AlO_4 tetrahedra in the glass without $C_{12}H_{22}O_{11}$, which is generally responsible for the loose glass structures. After adding $C_{12}H_{22}O_{11}$, the content of the oxygen decreases in the core of the bulk glass as a result of evolving gases from the two steps of reaction:

$$C_{12}H_{22}O_{11} \rightarrow C + 11H_2O$$

$$C + 2O \rightarrow CO_2$$

Part of the oxygen in reagents are consumed by the carbon from $C_{12}H_{22}O_{11}$. Compared with other main cation in the glass network, the coordination of Al would be affected in the first place. Thereby AlO_4 tetrahedra changes into AlO_6 octahedra, this can induce dense network, which is not conducive to the ion migration. So the crystallization is restrained in the glass added with $C_{12}H_{22}O_{11}$.

3.3. Crystallization kinetics

The crystallization kinetic characteristics of the glass can be determined by following Arrhenius [15], Kissinger [16] and Augis–Bennet [17], which are, respectively, expressed as:

$$k = \upsilon \exp\left(-\frac{E}{RT}\right) \quad (1)$$

$$\ln\left(\frac{T_p^2}{\alpha}\right) = \frac{E}{RT_p} + \ln\frac{E}{R} - \ln\upsilon \quad (2)$$

Table 2
T_p (K) values from DTA curve of glass samples at different heating rates.

Sample no.	$\alpha = 5$ (K min^{-1})	$\alpha = 10$ (K min^{-1})	$\alpha = 15$ (K min^{-1})	$\alpha = 20$ (K min^{-1})
A0	1113 ± 2	1127 ± 2	1138 ± 2	1147 ± 2
R0	1140 ± 2	1148 ± 2	1155 ± 2	1157 ± 2

$$n = \frac{2.5RT^2}{\Delta TE} \quad (3)$$

where T_p is the crystallization peak temperature with heating rate of α. E, R, υ and k are the activation energy for crystallization, the gas constant, the frequency factor, and the reaction rate constant, respectively. According to Eq. (1), a lower E value and a higher υ value correspond to a higher k, indicating a higher crystallization rate. ΔT is the half-height temperature wideness of the maximum exothermical peak of DTA. n is the crystallization index, which is related to crystallization manner, the crystallization manner is surface crystallization when n value is close to 1, two-dimension crystallization when n is close to 2 and volumetric crystallization when n is close to 3 [18].

Table 2 shows the crystallizing peak temperatures (T_p) from DTA curves at different heating rates. The DTA curves of R0 showed higher crystallization temperatures than that of sample A0, which is also an evidence of inhibited crystallization. The relationship between $\ln(T_p^2/\alpha)$ and $1/T_p$ is constructed (Fig. 9) to calculate the effective activation energy, frequency factor, and the reaction rate constant, as shown in Table 3. According to Kissinger's method, the plots should be linear, the slope of which represents the crystallization activation energy. The calculated activation energy of the A0 specimen without $C_{12}H_{22}O_{11}$ is 396.8 kJ/mol, while sample R0 with additional $C_{12}H_{22}O_{11}$ is determined to be 834.5 kJ/mol. The error limit marked in the Fig. 9 is the maximum deviation from the average value of the $\ln(T_p^2/\alpha)$.

Table 3
E, υ, n and k crystallization values of the glass samples.

Crystallization parameter	E (kJ/mol)	υ (min^{-1})	n	k ($\alpha = 5$ K min^{-1})
A0	396.8	8.8×10^{17}	0.95	0.2092
R0	834.5	6.6×10^{37}	1.38	0.3787

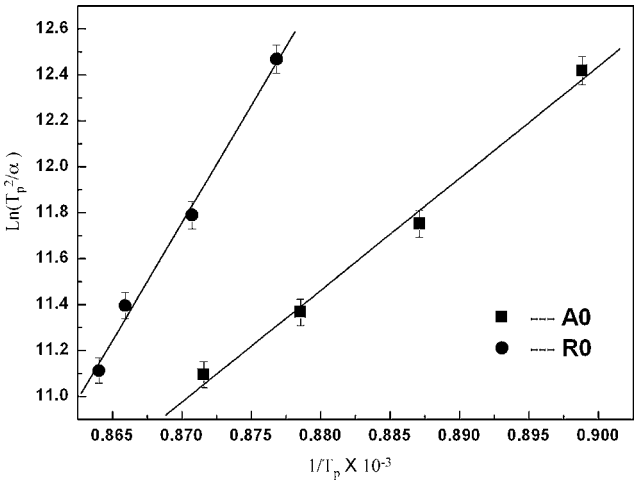

Fig. 9. Relationship between ln (T_p^2/α) and $1/T_p$ (error bar shows the maximum deviation from the average value).

The A0 specimen has much lower E and υ than R0. It is suggested that $C_{12}H_{22}O_{11}$ can increase the activation energy and frequency factor. The activation energy represented the energy barrier which must be overcome to transform the metastable glass phase into the more stable crystal phase. So it is extremely difficult for atoms to overcome the energy barrier and grow into diopside in the sample R0. This issue would obviously restrain the crystallization of CaO–MgO–SiO_2 glass.

At the heating rate of 5 K min^{-1}, the k values of glass containing $C_{12}H_{22}O_{11}$ is 0.3787, but the one without $C_{12}H_{22}O_{11}$ is only 0.2092. It is shown that the introduction of $C_{12}H_{22}O_{11}$ not only increases the activation energy and the frequency factor, but also increases the k values. This indicates that the $C_{12}H_{22}O_{11}$ restrained the crystallization of glass, but higher heat treatment temperature would help atoms in R0 specimen overcome the energy barrier, and then the crystal would grow at a higher crystallization rate.

The n values, which are calculated by using Eq. (3), are also given in Table 3. The fact that n values is near 1 indicates that crystallization manner of CaO–MgO–SiO_2 glass is surface crystallization. The n values of A0 and R0 specimens are 0.95 and 1.38, respectively, suggested that the crystallization manner changes from surface crystallization to two-dimension crystallization, which match well with the results of SEM.

4. Conclusions

The production of glass ceramics based on the CaO–MgO–SiO_2 system using additives $C_{12}H_{22}O_{11}$ confirmed the influence of reductant on the crystallization. The results of this study are summarized as follows:

(1) The addition of $C_{12}H_{22}O_{11}$ to the CaO–MgO–SiO_2 glass inhibits the surface crystallization of the diopside phase. After adding $C_{12}H_{22}O_{11}$, the crystal content and crystalline layer thickness of glass ceramics decreased.
(2) The microstructure of the bulk glass ceramics showed that the investigated glass were prone to surface crystallization. The EDS indicated that the inhibited crystallization was caused by the lack of oxygen in the core of the glass added $C_{12}H_{22}O_{11}$.
(3) The kinetic analysis indicated that the $C_{12}H_{22}O_{11}$ played an important role in adjusting the crystallization kinetic parameters of CaO–MgO–SiO_2 glass.

Acknowledgement

The authors would like to thank Professor Qiming Liu and Dr. Haizheng Tao for their helpful discussion.

References

[1] C. Fredericci, E.D. Zanotto, E.C. Ziemath, J. Non-Cryst. Solids 273 (2000) 64–75.
[2] P. Alizadeh, V.K. Marghussian, J. Eur. Ceram. Soc. 20 (2000) 765–773.
[3] T. Kokubo, S. Ito, S. Sakka, J. Mater. Sci. 21 (1986) 536–540.
[4] J. Cheng, P. Tian, L. Tang, et al., J. Chn. Ceram. Soc. 36 (2008) 1017–1021.
[5] J. Cheng, P. Tian, W. Zheng, et al., J. Alloys Compd. 471 (2009) 470–473.
[6] J. Fu, J. Am. Ceram. Soc. 83 (2000) 2613–2615.
[7] F. Qin, C. Chang, D. Mao, J. Alloys Compd. 390 (2005) 133–137.
[8] L. Jiang, C. Chang, D. Mao, et al., J. Alloys Compd. 377 (2004) 211–215.
[9] P. Alizadeh, M. Yousefi, B. Eftekhari Yekta, et al., Ceram. Int. 33 (2007) 767–771.
[10] M. Rezvani, B. Eftekhari Yekta, V.K. Marghussian, J. Eur. Ceram. Soc. 25 (2005) 1525–1530.
[11] D.U. Tulyagano, S. Agathopoulos, J.M. Ventura, et al., J. Eur. Ceram. Soc. 26 (2006) 1463–1471.
[12] R. Müller, E.D. Zanotto, V.M. Fokin, J. Non-Cryst. Solids 274 (2000) 208–231.
[13] S. Agathopoulos, D.U. Tulyaganov, J.M.G. Ventura, et al., J. Non-Cryst. Solids 352 (2006) 322–328.
[14] G. Partridge, P.W. McMillan, Glass Technol. 15 (1974) 127–133.
[15] M. Avrami, J. Chem. Phys. 7 (1939) 1102–1103.
[16] H.E. Kissinger, J. Res. Nat. Bur. Stand. 57 (1956) 217–221.
[17] J.A. Augis, J.E. Bennett, J. Therm. Anal. 13 (1978) 283–292.
[18] X.Z. Guo, H. Yang, M. Cao, Therm. Acta 444 (2006) 201–205.